ELSEVIER

Thermochimica Acta 296 (1997) 129–134

thermochimica acta

# Studies on the non-isothermal kinetics of thermal decomposition of the complex of europium *p*-methylbenzoate with 2,2′-dipyridine

Ping Mu[a,*], RuiFen Wang[b], Liang Zhao[c]

[a]*Experimental Center, Hebei Teachers' University, Shijiazhuang, 050016, People's Republic of China*
[b]*Department of Chemistry, Hebei Normal College, Shijiazhuang, 050091, People's Republic of China*
[c]*Department of Computer Science, Hebei Teachers' University, Shijiazhuang, 050016, People's Republic of China*

Received 10 February 1996; received in revised form 7 March 1996; accepted 10 December 1996

**Abstract**

Thermal decomposition of the complex of europium *p*-methylbenzoate with 2,2′-dipyridine and its kinetics were studied under the non-isothermal condition by TG and DTG techniques. The non-isothermal kinetic data were analyzed by means of the Achar method and the Coats–Redfern method. The possible reaction mechanisms were suggested by comparing the kinetic parameters. The kinetic equation for the first stage can be expressed as:

$$d\alpha/dt = A\exp(-E/RT)\,3/2(1+\alpha)^{2/3}\,[(1+\alpha)^{1/3}-1]^{-1},$$

while for the third stage, $d\alpha/dt = A\exp(-E/RT)(1-\alpha)$. Mathematic expressions were derived from the kinetic compensation effects. © 1997 Elsevier Science B.V.

*Keywords:* Eu(III) complex; Thermal decomposition; Non-isothermal kinetics

## 1. Introduction

The special structure and the interesting luminescent character of the Eu(III) complex made it very important in applied researches as well as in theoretical studies.

Based on the preparation and the determination of the crystal structure and luminescence spectra of the complex [1], we have studied the non-isothermal kinetic data by means of the Achar method and the Coats–Redfern method and have suggested the possible reaction mechanism.

## 2. Experimental

### 2.1. Sample

The complex of europium *p*-methylbenzoate with 2,2′-dipyridine was prepared as described previously [1].

### 2.2. Apparatus

Decomposition experiments of Eu(*p*-MBA)$_3$ dipy (*p*-MBA: *p*-methylbenzoate and dipy: 2,2′-dipyridine) were carried out using a Perkin–Elmer TGA7 thermogravimetric analyzer under a nitrogen atmosphere, at a

*Corresponding author.


*PII* S0040-6031(97)00014-2

flow rate of 40 ml $min^{-1}$. The heating rate used was 10°C $min^{-1}$ from ambient to 840°C and sample sizes were 3±0.1 mg.

## 3. Results and discussion

### 3.1. Thermal decomposition

The TG and DTG curves of Eu(*p*-MBA)$_3$ dipy are shown in Fig. 1. The thermoanalytical data for the complex are given in Table 1.

The Eu(III) complex decomposed via intermediates to give the europium oxide as an end product. The percentage of mass loss and probable compositions of the expelled groups are also listed in Table 1. The results of thermal analysis indicate that the complex undergoes a three-stage decomposition process. The TG–DTG curves show degradation in the first stage at in the 168–243°C temperature range and a dipy was considered to be expelled with a mass loss of 21.92% (theoretical loss is 21.89%). The degradation can also be demonstrated by the bond distances of the structure of the complex (Fig. 2). Eu–N distance is longer than any other bond distance; theoretically speaking, this bond is less stable and easy broken down. The second-stage degradation temperature is in the range 243–487°C with the mass loss of 19.10%, which is nearly equal to the theoretical loss of 18.94% which is the value of removal of one ion of *p*-MBA. Actually, this stage decomposition includes two steps in which the first step is in the range 243–457°C and second step is in the range 457–487°C with two intermediates of $Eu_2(CH_3C_6H_4COO)_4O_2$ and $[Eu_2(CH_3C_6H_4COO)_4]^{2+}$, obtained separately. This

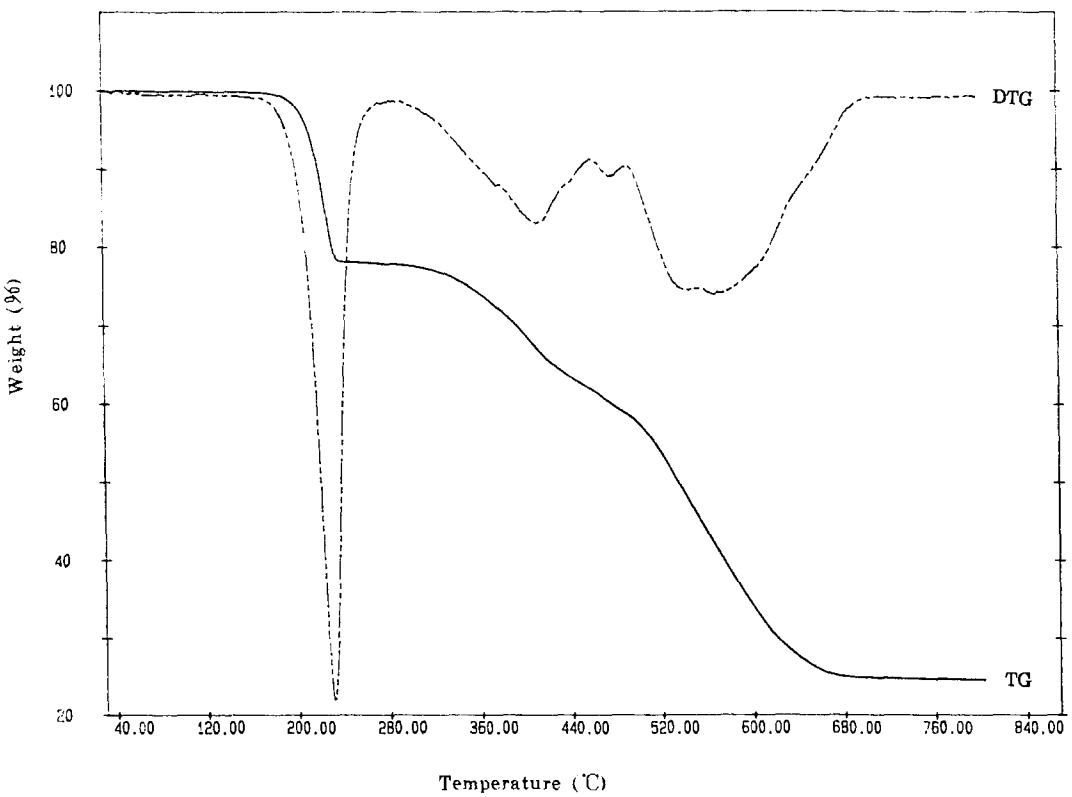


Fig. 1. Thermogravimetric curves (DTG and TG) for Eu(*p*-MBA)$_3$ dipy.

Table 1
Thermal decomposition data for Eu(*p*-MBA)$_3$ dipy [$Eu_2(CH_3C_6H_4COO)_6(C_{10}H_8N_2)_2$] from TG and DTG analyses

| Decomposition Temperature range (°C) | Loss of mass (wt%) | | Probable composition of expelled group | Intermediate |
|---|---|---|---|---|
| | TG | Theory | | |
| 168–243 | 21.92 | 21.89 | $-2C_{10}H_8N_2$ | $Eu_2(CH_3C_6H_4COO)_6$ |
| 243–457 | 16.20 | 16.70 | $-2C_8H_7O$ | $Eu_2(CH_3C_6H_4COO)_4O_2$ |
| 457–487 | 2.90 | 2.24 | $-O_2$ | $[Eu_2(CH_3C_6H_4COO)_4]^{2+}$ |
| 487–680 | 34.54 | 34.51 | $-C_{32}H_{28}O_5$ | $Eu_2O_3$ |

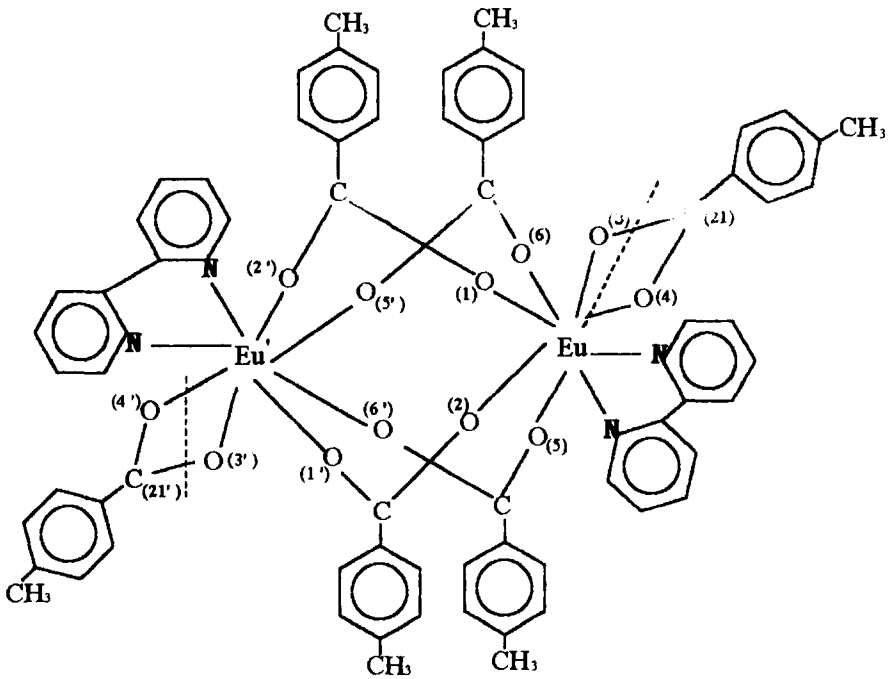


Fig. 2. Structure and partial data of bond distances of Eu(*p*-MBA)$_3$ dipy [1].

degradation process can also be explained by structural data. From Fig. 2,

| | distance ($\times 10^{-1}$ nm) |
|---|---|
| [1]Eu–O(1) | 2.385 |
| Eu–O(2) | 2.315 |
| Eu–O(3) | 2.439 |
| Eu–O(4) | 2.500 |
| Eu–O(5) | 2.446 |
| Eu–O(6) | 2.330 |
| Eu–N(1) | 2.655 |
| Eu–N(2) | 2.618 |

[1]Eu′–O and Eu′–N bond is the same as Eu–O and Eu–N bond.

| | |
|---|---|
| O(3)–C(21) | 1.301 |
| O(4)–C(21) | 1.24 |

we can see that the distance of Eu–O(4) is the longest among all Eu–O bonds. Also, O(3) and O(4) are connected with C(21), the bond distance O(3)–C(21) = 1.301 > O(4)–C(21) = 1.24. Thus, Eu–O(4) and O(3)–C(21) bonds were considered to be broken down following the Eu–N bond, as indicated by the broken line in Fig. 2. The intermediate, $Eu_2(CH_3C_6H_4COO)_4O_2$, was produced with a mass loss of 16.2% (theoretical loss 16.7%). But there is no clear plateau in the TG curve, it continues to lose weight. TG curve indicates that with the rise of temperature, $Eu_2(CH_3C_6H_4COO)_4O_2$ continues to

degrade – remove $O_2$ and turn into $[Eu_2(CH_3C_6H_4COO)_4]^{2+}$. This degradation was followed by the third stage of decomposition in the 487–680°C temperature range, in which the other two ions of *p*-MBA were removed with a mass loss of 34.54% (theoretical loss is 34.51%). Up to now, the Eu(III) complex were completely degraded into $Eu_2O_3$, with a total loss of 75.56% (theoretical loss is 75.34%).

In base of above inference, the thermal decomposition process of Eu(III) complex may be expressed by the following scheme:

$$Eu_2(CH_3C_6H_4COO)_6(C_{10}H_8N_2)_2 \rightarrow Eu_2(CH_3C_6H_4COO)_6 \rightarrow Eu_2(CH_3C_6H_4COO)_4O_2 \rightarrow [Eu_2(CH_3C_6H_4COO)_4]^{2+} \rightarrow Eu_2O_3$$

Table 2
Basic data for Eu(*p*-MBA)$_3$ dipy determined by TG and DTG

| Stage 1 | | | | Stage 3 | | | |
|---|---|---|---|---|---|---|---|
| No. | $\alpha$ | $T$ per K | d$\alpha$/d$T$ | No. | $\alpha$ | $T$ per K | d$\alpha$/d$T$ |
| 1 | 0.013 | 443.14 | 0.099 | 1 | 0.0487 | 770.65 | 1.124 |
| 2 | 0.0153 | 448.14 | 0.124 | 2 | 0.1074 | 783.12 | 1.685 |
| 3 | 0.0194 | 453.14 | 0.187 | 3 | 0.1877 | 795.64 | 2.231 |
| 4 | 0.0262 | 458.14 | 0.287 | 4 | 0.2792 | 808.15 | 2.512 |
| 5 | 0.0374 | 463.14 | 0.449 | 5 | 0.3157 | 813.12 | 2.549 |
| 6 | 0.0554 | 468.14 | 0.699 | 6 | 0.3521 | 818.14 | 2.512 |
| 7 | 0.0839 | 473.14 | 1.061 | 7 | 0.406 | 825.62 | 2.524 |
| 8 | 0.1279 | 478.14 | 1.624 | 8 | 0.4423 | 830.65 | 2.543 |
| 9 | 0.195 | 483.14 | 2.436 | 9 | 0.4792 | 835.62 | 2.580 |
| 10 | 0.294 | 488.14 | 3.587 | 10 | 0.5163 | 840.65 | 2.593 |
| 11 | 0.4339 | 493.14 | 5.083 | 11 | 0.5344 | 843.13 | 2.587 |
| 12 | 0.6184 | 498.14 | 6.744 | 12 | 0.5889 | 850.64 | 2.556 |
| 13 | 0.7221 | 500.64 | 7.456 | 13 | 0.6413 | 858.14 | 2.487 |
| 14 | 0.8248 | 503.14 | 7.798 | 14 | 0.7239 | 870.65 | 2.331 |
| 15 | 0.9123 | 505.64 | 7.509 | 15 | 0.7997 | 883.15 | 2.125 |
| 16 | 0.971 | 508.14 | 6.474 | 16 | 0.8626 | 895.65 | 1.756 |
| 17 | 0.9948 | 510.64 | 4.975 | 17 | 0.9097 | 908.15 | 1.374 |
| | | | | 18 | 0.9479 | 920.65 | 1.113 |
| | | | | 19 | 0.9771 | 933.14 | 0.849 |
| | | | | 20 | 0.9952 | 945.64 | 0.531 |

Table 3
The common forms of $f(\alpha)$ and $g(\alpha)$

| Function No. | $g(\alpha)$ | $f(\alpha)$ |
|---|---|---|
| 1 | $\alpha^2$ | $1/(2\alpha)$ |
| 2 | $\alpha+(1-\alpha)\ln(1-\alpha)$ | $-[\ln(1-\alpha)]^{-1}$ |
| 3 | $(1-2\alpha/3)-(1-\alpha)^{2/3}$ | $3/2[(1-\alpha)^{-1/3}-1]^{-1}$ |
| 4 | $[1-(1-\alpha)^{1/3}]^2$ | $3/2(1-\alpha)^{2/3}[1-(1-\alpha)^{1/3}]^{-1}$ |
| 5 | $[(1+\alpha)^{1/3}-1]^2$ | $3/2(1+\alpha)^{2/3}[(1+\alpha)^{1/3}-1]^{-1}$ |
| 6 | $[1/(1-\alpha)^{1/3}-1]^2$ | $3/2(1-\alpha)^{4/3}[1/(1-\alpha)^{1/3}-1]^{-1}$ |
| 7 | $-\ln(1-\alpha)$ | $(1-\alpha)$ |
| 8–11 | $[-\ln(1-\alpha)]^n$ ($n$ = 2/3, 1/2, 1/3 and 1/4) | $1/n(1-\alpha)[-\ln(1-\alpha)]^{-(n-1)}$ |
| 12–13 | $1-(1-\alpha)^n$ ($n$ = 1/2 and 1/3) | $1/n(1-\alpha)^{-(n-1)}$ |
| 14–17 | $\alpha^n$ ($n$ = 1, 1/2, 1/3 and 1/4) | $1/n\alpha^{-(n-1)}$ |
| 18 | $(1-\alpha)^{-1}-1$ | $(1-\alpha)^2$ |
| 19 | $(1-\alpha)^{-1/2}$ | $2(1-\alpha)^{3/2}$ |

### 3.2. Kinetic studies of non-isothermal decomposition

In the present paper, we use the Achar [2] method and the Coats–Redfern [3] method to study the kinetics of the first and third decomposition process of the complex.

The integral and differential equations are as follows:

$$\ln[(d\alpha/dt)/f(\alpha)] = \ln A - E/RT, \quad (1)$$

$$\ln[g(\alpha)/T^2] = \ln AR/\beta E - E/RT, \quad (2)$$

where $\alpha$ is the fractional decomposition, $T$ is the absolute temperature, $A$ is the pre-exponential factor, $R$ is the gas constant in kJ mol$^{-1}$°C$^{-1}$, $E$ is the apparent activation energy (kJ mol$^{-1}$), $\beta$ is the heating rate in °C min$^{-1}$, $f(\alpha)$ and $g(\alpha)$ are the differential and integral mechanism functions, respectively.

The basic parameters, $\alpha$, $T$ and $d\alpha/dt$, were obtained from the TG and DTG curves (listed in Table 2). With use of the common forms of $f(\alpha)$ and $g(\alpha)$, in Table 3, the kinetic analysis were completed with the linear least squares method and the results are showed in Tables 4 and 5. When the values of $E$ and $A$ obtained with the two methods are approximately the same and the linear correlation coefficient is better, it can be concluded that the relevant function is the function of the probable thermal decomposition mechanism of the complex.

For the first stage of decomposition of the complex, it can be suggested that the function of the possible mechanism is function No. 5 in Table 3 based on the data in Table 4. The decomposition reaction was governed by three-dimensional diffusion (the Anti–Jander equation). The kinetic equation of this process is:

$$d\alpha/dt = A\exp(-E/RT)\,3/2(1+\alpha)^{2/3} \cdot [(1+\alpha)^{1/3} - 1]^{-1}.$$

Table 5 shows that the values of $E$ and $A$ obtained by the two methods are almost the same and the value of $r$ is better when the function is function No. 7 in Table 3. It can be concluded that the decomposition in the third stage conformed to the Avrami–Erofeev equation. The kinetic equation is:

$$d\alpha/dt = A\exp(-E/RT)(1-\alpha).$$

Via the mathematical expression for the kinetic compensation effect, $\ln A = aE + b$ [4], where $\ln A$

Table 4
Kinetic parameter for the thermal decomposition data of Eu($p$-MBA)$_3$ dipy: Stage 1

| Function No. | Integral method | | | Differential method | | |
|---|---|---|---|---|---|---|
| | $E$ (kJ mol$^{-1}$) | ln $A$ (s$^{-1}$) | $r$ | $E$ (kJ mol$^{-1}$) | ln $A$ (s$^{-1}$) | $r$ |
| 1 | 262.808 | 62.454 | 0.995 | 265.716 | 65.853 | 0.993 |
| 2 | 279.500 | 66.201 | 0.995 | 299.826 | 74.087 | 0.998 |
| 3 | 287.070 | 66.705 | 0.995 | 316.704 | 76.991 | 0.997 |
| 4 | 303.250 | 70.993 | 0.993 | 347.472 | 85.030 | 0.990 |
| 5 | 247.823 | 56.243 | 0.996 | 244.215 | 57.979 | 0.990 |
| 6 | 364.785 | 87.256 | 0.973 | 439.774 | 109.147 | 0.956 |
| 7 | 161.550 | 38.832 | 0.985 | 222.650 | 57.213 | 0.961 |
| 8 | 105.058 | 24.738 | 0.985 | 166.157 | 43.144 | 0.948 |
| 9 | 76.811 | 17.593 | 0.984 | 137.911 | 36.025 | 0.936 |
| 10 | 48.565 | 10.303 | 0.982 | 109.664 | 28.788 | 0.916 |
| 11 | 34.442 | 6.543 | 0.980 | 95.541 | 25.084 | 0.900 |
| 12 | 141.769 | 32.835 | 0.994 | 176.499 | 44.462 | 0.993 |
| 13 | 147.661 | 34.012 | 0.992 | 191.883 | 48.076 | 0.984 |
| 14 | 127.440 | 29.667 | 0.995 | 130.384 | 33.096 | 0.983 |
| 15 | 59.756 | 12.878 | 0.995 | 62.664 | 16.372 | 0.942 |
| 16 | 37.195 | 7.060 | 0.994 | 40.102 | 10.622 | 0.877 |
| 17 | 25.914 | 4.027 | 0.993 | 28.822 | 7.663 | 0.796 |
| 18 | 219.742 | 54.329 | 0.932 | 314.952 | 81.330 | 0.902 |
| 19 | 38.223 | 8.458 | 0.661 | 268.801 | 68.579 | 0.929 |

Table 5
Kinetic parameter for the thermal decomposition data of Eu(*p*-MBA)$_3$ dipy: Stage 3

| Function No. | Integral method | | | Differential method | | |
|---|---|---|---|---|---|---|
| | $E$ (kJ mol$^{-1}$) | ln $A$ (s$^{-1}$) | $r$ | $E$ (kJ mol$^{-1}$) | ln $A$ (s$^{-1}$) | $r$ |
| 1 | 159.861 | 19.731 | 0.892 | 57.338 | 8.648 | 0.555 |
| 2 | 183.889 | 22.863 | 0.922 | 110.417 | 15.996 | 0.845 |
| 3 | 195.692 | 23.209 | 0.936 | 138.513 | 18.706 | 0.920 |
| 4 | 221.133 | 27.179 | 0.958 | 189.051 | 26.302 | 0.973 |
| 5 | 142.762 | 14.699 | 0.875 | 33.111 | 2.585 | 0.372 |
| 6 | 322.21 | 42.746 | 0.990 | 340.666 | 49.088 | 0.980 |
| 7 | 125.905 | 16.000 | 0.978 | 121.919 | 19.207 | 0.960 |
| 8 | 79.201 | 9.011 | 0.975 | 75.215 | 12.276 | 0.899 |
| 9 | 55.849 | 5.399 | 0.971 | 51.862 | 8.726 | 0.806 |
| 10 | 32.496 | 1.595 | 0.962 | 28.510 | 5.058 | 0.581 |
| 11 | 20.820 | −0.482 | 0.948 | 16.834 | 3.139 | 0.380 |
| 12 | 94.230 | 10.38 | 0.934 | 46.111 | 7.120 | 0.923 |
| 13 | 103.462 | 11.323 | 0.951 | 71.381 | 10.513 | 0.966 |
| 14 | 72.826 | 7.411 | 0.873 | −29.696 | −3.580 | 0.537 |
| 15 | 29.309 | 0.733 | 0.819 | −73.213 | −10.040 | 0.934 |
| 16 | 14.804 | −1.872 | 0.730 | −87.719 | −12.368 | 0.969 |
| 17 | 7.551 | −3.507 | 0.584 | −94.972 | −13.617 | 0.978 |
| 18 | 224.442 | 31.322 | 0.977 | 273.534 | 41.993 | 0.933 |
| 19 | 61.600 | 7.102 | 0.861 | 197.727 | 29.907 | 0.943 |

and $E$ were obtained with integral and differential methods (the data was listed in Tables 4 and 5). Computation with the linear least squares method on a computer yields the kinetic compensation parameters $a$ and $b$. The mathematic expression for the kinetic compensation effect of the first stage is: $\ln A = 0.2412E - 1.3223$ and $r = 0.9993$. The mathematic expression of the third stage is: $\ln A = 0.1431E - 3.3022$ and $r = 0.9957$.

## References

[1] R.F. Wang, L.P. Jin, M.Z. Wang, S.H. Huang and X.T. Chen, Acta Chimica Sinica (in Chinese), 53 (1995) 39–45.
[2] B.N. Achar, Proc. Int. Clay Conf, Jerusalem, 1 (1966) 67.
[3] A.W. Coats and J.D. Redfern, Nature, 201 (1964) 68.
[4] J. Zsako, J. Thermal. Anal., 9 (1976) 101.